

Thermal Crosstalk Effects in a Silicon Photonics Neuromorphic Network

*Original*

Thermal Crosstalk Effects in a Silicon Photonics Neuromorphic Network / Orlandin, Marco; Cem, Ali; Curri, Vittorio; Carena, Andrea; Ros, Francesco Da; Bardella, Paolo. - 2023-September:(2023), pp. 43-44. ( 23rd International Conference on Numerical Simulation of Optoelectronic Devices, NUSOD 2023 Torino (Ita) 18-21 September 2023) [10.1109/nusod59562.2023.10273549].

*Availability:*

This version is available at: 11583/3005755 since: 2025-12-10T15:18:14Z

*Publisher:*

IEEE

*Published*

DOI:10.1109/nusod59562.2023.10273549

*Terms of use:*

This article is made available under terms and conditions as specified in the corresponding bibliographic description in the repository

*Publisher copyright*

(Article begins on next page)

# Thermal Crosstalk Effects in a Silicon Photonics Neuromorphic Network

Marco Orlandin\*, Ali Cem†, Vittorio Curri\*, Andrea Carena\*, Francesco Da Ros†, Paolo Bardella\*

\*Department of Electronics and Communications, Politecnico di Torino, Turin, Italy

Email: paolo.bardella@polito.it

†Department of Electrical and Photonics Engineering, Technical University of Denmark, Denmark

Email: fdro@dtu.dk

**Abstract**—We propose a methodology to include thermal crosstalk effects in the modeling of neuromorphic photonic circuits. Through component-level simulations of device building blocks and thermal analysis, we are able to successfully account for thermal effects, as shown by a comparison with experimental measurements of a  $3 \times 3$  programmable optical circuit.

**Index Terms**—Integrated photonics, silicon photonics, thermal effects, thermal crosstalk.

## I. INTRODUCTION

Neuromorphic silicon photonic circuits represent an important development in the field of artificial intelligence for their ability to process information in the optical domain quickly and accurately, in a programmable way, and with improved energy efficiency compared to traditional computing systems [1]. However, the design and analysis of these devices can be challenging, in particular due to the large number of integrated components that are present, and the real behavior of the circuit can differ significantly from the expected one due to non-idealities in the components, realization tolerances [2], and tuning issues. In fact, since thermal tuning is generally used to control the behavior of the device and select the operation that it must perform, particular attention must be paid to properly take into account thermal and electrical crosstalk, which could significantly degrade overall performance [3], [4]. Although the thermal problem could be addressed by increasing the distances between MZIs or creating proper isolation trenches, these solutions result in an increased footprint or more complex fabrication steps and reduce the number of photonic devices that can be integrated into a single chip. To maintain the large-scale integration typical of photonic components, we propose a more effective approach in which a self-consistent numerical analysis is carried out to effectively include thermal crosstalk in the control strategy. The analysis is divided into three main steps: first, a component-level study with finite-difference time-domain (FDTD), then an electrothermal analysis, and finally a system-level evaluation of the transmission properties of the whole device. This approach is successfully applied to the analysis of an experimentally characterized device.

## II. REFERENCE DEVICE

The reference device analysed in this work is a portion of a larger optical reconfigurable switch operating in the C band,

designed at the Department of Photonics Engineering of the Technical University of Denmark (DTU) [5], [6]. Details on the fabrication of this silicon photonic chip are given in [7]. A reference schematic of the circuit analyzed is shown in Fig. 1; there, the three output optical powers ( $P_{out1}-P_{out3}$ ) are linear combinations of the three input optical signals ( $P_{in1}-P_{in3}$ ), with weights that can be dynamically modified according to the voltages applied to one arm of the nine Mach-Zehnder interferometers (MZIs) based on two  $2 \times 2$  Multi Mode Interferometers (MMIs). Experimental characterizations of the network have been carried out at DTU, injecting a signal into one port and measuring the powers at three output ports. As an example, the results obtained when the input signal is injected at port 1 and the output is measured at port 2 ( $P_{out,2}/P_{in,1}$ ) are shown by the red line in Fig. 2; in each interval delimited by the dashed lines, the control voltage of the MZI indicated at the bottom is tuned between 0 V and 2 V (theoretically corresponding to a  $180^\circ$  change in the upper MZI arm) with 11 uniform steps, while the control voltages of the other MZIs are set to 0 V [8], [9]. A preliminary analysis of the circuit, where the input powers are propagated to the output considering an ideal behavior of all of the MZIs and neglecting optical losses, results in the behavior described by the dashed blue line, which differs significantly from the measured evidence.

## III. RESULTS

Based on FDTD simulations in Synopsys RSoft<sup>®</sup>, a first study is performed of the  $500 \text{ nm} \times 250 \text{ nm}$  waveguide, the MMI and the crossing, to extract the optical losses associated to each fundamental block. For the MZIs simulations are also used to precisely calculate the distribution of optical power at the two outputs as a function of the phase shift in one of the branches. Examples of these analyses are reported in Fig. 3.

Moving to the thermal analysis, in the proposed device the thermal adjustment is obtained thanks to a thermo-optical

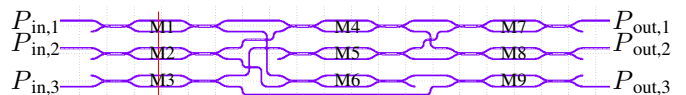


Fig. 1. Detail of the  $3 \times 3$  considered circuit. Labels M1–M9 identify the nine MZIs. The overall dimension is approximately  $1800 \mu\text{m} \times 300 \mu\text{m}$ . The red line indicates the position of the cross-section used in Fig. 4.

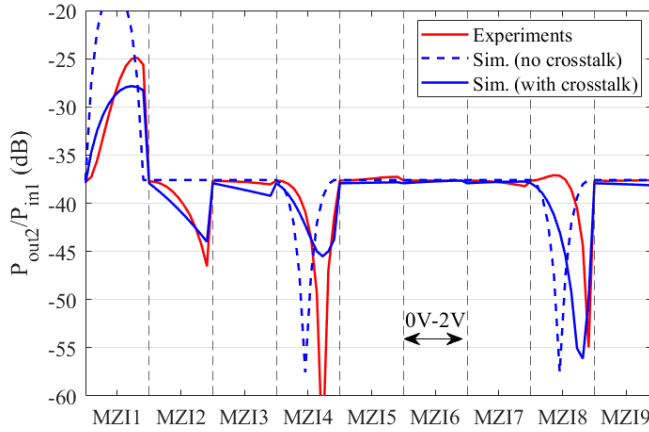


Fig. 2. Power at output port 2 with input signal at port 1, as a function of the MZIs' voltages: experiments (red), simulation without crosstalk (dashed blue), and simulation including crosstalk (blue). In each interval delimited by vertical dashed lines, the voltage of the mZi indicated at the bottom is tuned between 0 V and 2 V, while the voltage of the other MZIs is 0 V.

phase shifter (TOPS) with a resistive titanium heater, with  $0.1 \mu\text{m}$  thickness,  $1.8 \mu\text{m}$  width, and  $10 \mu\text{m}$  length, placed on top of the waveguide separated by an oxide layer. The lower part of the chip is supposed to be kept at  $20^\circ\text{C}$ . We focus on a group of three vertically adjacent MZIs, since the horizontal distance between the MZIs is greater than  $500 \mu\text{m}$ . Thermal analysis is performed with COMSOL Multiphysics<sup>®</sup> considering a  $1 \text{ mm}$  long,  $1.2 \text{ mm}$  wide, and  $1 \text{ mm}$  deep 3D box with six waveguides, three of which have a heater on top. Parametric analyzes are performed to correlate the heaters' voltages to the temperature variation and quantify the crosstalk. As an example, Fig. 4 shows the distribution of temperature in a cross section at the center of the heaters (red line in Fig. 1) and at the same height of the waveguides; 2 V are applied to the heater of MZI1. Although the heater successfully increases to  $70^\circ\text{C}$  the temperature of the waveguide immediately below, the second arm of the same MZI is also significantly heated ( $32^\circ\text{C}$ ), with a substantial reduction in the overall optical phase difference between the two arms. Furthermore, MZI2

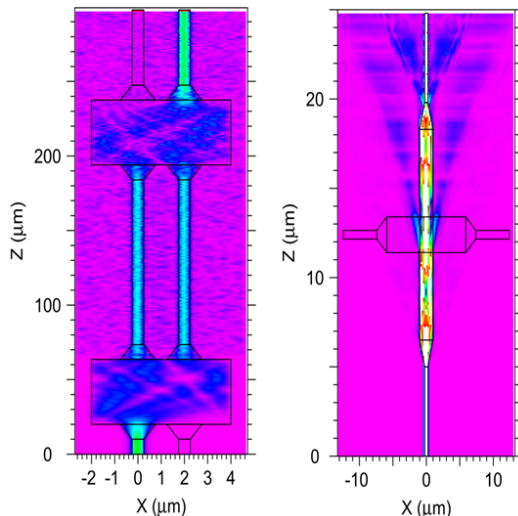


Fig. 3. FDTD simulations of a MZI (left) and a waveguide crossing (right).

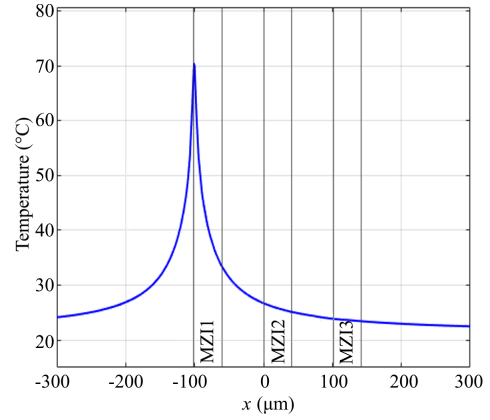


Fig. 4. Cross section of the temperature distribution in the position indicated by the red line in Fig. 1, at the waveguides height, when a 2 V control voltage is applied to the heater of MZI1. The thicker vertical lines indicate the position of the waveguides.

waveguides also experience significant temperature variation. The estimated temperature distribution is used to calculate an effective index variation [10] in the six waveguides.

The information extracted from the FDTD analysis and the calculated thermal effects are used to refactor the calculation of the output power; as shown by the continuous blue curve in Fig.2 the model is now able to predict with improved accuracy the experimental findings; the remaining discrepancy can be mainly attributed to electrical interconnections crosstalk, not yet included in the model.

#### IV. CONCLUSIONS

We proposed a methodology to model thermal crosstalk in integrated photonic circuits. The approach starts with an FDTD analysis of the basic components, followed by a thermal analysis of the region below the heaters. The results are used to drive a system-level simulation of the device, which is able to predict with improved accuracy the device output. The method has been applied successfully to describe the behavior of a  $3 \times 3$  programmable optical circuit.

#### REFERENCES

- [1] B. J. Shastri *et al.*, "Photonics for artificial intelligence and neuromorphic computing," *Nat. Photonics*, vol. 15, no. 2, pp. 102–114, Feb 2021.
- [2] M. Y.-S. Fang *et al.*, "Design of optical neural networks with component imprecisions," *Opt. Express*, vol. 27, no. 10, pp. 14 009–14 029, 2019.
- [3] D. Pérez *et al.*, "Multipurpose silicon photonics signal processor core," *Nat. Commun.*, vol. 8, no. 1, p. 636, Sep 2017.
- [4] S. Bandyopadhyay *et al.*, "Hardware error correction for programmable photonics," *Optica*, vol. 8, no. 10, pp. 1247–1255, Oct 2021.
- [5] M. A. Nahmias *et al.*, "Photonic multiply-accumulate operations for neural networks," *IEEE J. Sel. Top. in Quantum Electron.*, vol. 26, no. 1, pp. 1–18, 2020.
- [6] L. De Marinis *et al.*, "Photonic integrated reconfigurable linear processors as neural network accelerators," *Appl. Sci.*, vol. 11, no. 13, 2021.
- [7] Y. Ding *et al.*, "Reconfigurable sdm switching using novel silicon photonic integrated circuit," *Sci. Rep.*, vol. 6, no. 1, p. 39058, Dec 2016.
- [8] A. Cem *et al.*, "Comparison of models for training optical matrix multipliers in neuromorphic pics," in *2022 Optical Fiber Communications Conference and Exhibition (OFC)*, 2022, pp. 1–3.
- [9] —, "Data-driven modeling of Mach-Zehnder interferometer-based optical matrix multipliers," *J. Light. Technol.*, p. 12, 2023.
- [10] H. H. Li, "Refractive index of silicon and germanium and its wavelength and temperature derivatives," *J. Phys. Chem. Ref. Data*, vol. 9, no. 3, pp. 561–658, 07 1980.